Disorder-Driven Metal-Insulator Transitions in Deformable Lattices

Domenico Di Sante,[1,2] Simone Fratini,[3] Vladimir Dobrosavljević,[4] and Sergio Ciuchi[5,6]
[1]Institute of Physics and Astrophysics, University of Würzburg, Würzburg, Germany
[2]Consiglio Nazionale delle Ricerche (CNR-SPIN), Via Vetoio, L'Aquila, Italy
[3]Institut Néel-CNRS and Université Grenoble Alpes, Boîte Postale 166, F-38042 Grenoble Cedex 9, France
[4]Department of Physics and National High Magnetic Field Laboratory, Florida State University, Tallahassee, Florida 32306, USA
[5]Department of Physical and Chemical Sciences, University of L'Aquila, Via Vetoio, L'Aquila, Italy I-67100
[6]Consiglio Nazionale delle Ricerche (CNR-ISC) Via dei Taurini, Rome, Italy I-00185
(Received 13 May 2016; revised manuscript received 5 December 2016; published 20 January 2017)

We show that, in the presence of a deformable lattice potential, the nature of the disorder-driven metal-insulator transition is fundamentally changed with respect to the noninteracting (Anderson) scenario. For strong disorder, even a modest electron-phonon interaction is found to dramatically renormalize the random potential, opening a mobility gap at the Fermi energy. This process, which reflects disorder-enhanced polaron formation, is here given a microscopic basis by treating the lattice deformations and Anderson localization effects on the same footing. We identify an intermediate "bad insulator" transport regime which displays resistivity values exceeding the Mott-Ioffe-Regel limit and with a negative temperature coefficient, as often observed in strongly disordered metals. Our calculations reveal that this behavior originates from significant temperature-induced rearrangements of electronic states due to enhanced interaction effects close to the disorder-driven metal-insulator transition.

DOI: 10.1103/PhysRevLett.118.036602

Introduction.—Sufficiently strong disorder typically leads to the formation of bound electronic states. This physical process—Anderson localization—is by now well understood in the noninteracting limit [1,2]. Still, even early experimental and theoretical studies stressed [3] that omnipresent interaction effects cannot be disregarded, although they proved difficult to tackle. From the theoretical point of view, the pitfall of conventional weak-coupling theories has been the challenge in incorporating the strong interaction effects at the same level as disorder, especially in compounds with local magnetic moments and various Mott systems. The theoretical landscape changed dramatically following the rise of dynamical mean-field theory (DMFT) ideas [4], which provided a new perspective. Several intriguing phenomena, such as disorder-driven non-Fermi liquid behavior [5], glassy dynamics of electrons [6], and even the physics of Mott-Anderson transitions [7] have been captured, with the focus on systems with strong electronic correlations.

Many other materials, including the famous $A15$ compounds [8], as well as "phase-changing" amorphous alloys [9], can be experimentally tuned through disorder-driven metal-insulator transitions (MITs) [10,11], but they often do not display [3] strong electronic correlations of the Mott type [7]. In many such systems, transport on the metallic side is dominated by conventional electron-phonon scattering, leading to familiar linear resistivity at ambient temperatures. This behavior is modified as disorder increases, leading to a change of sign in the temperature coefficient of resistivity (TCR), and eventually a crossover to the insulating behavior. While the precise mechanism has long remained a puzzle [3], one thing is clear: the relevant transport processes must reflect a nontrivial interplay of the dynamical lattice deformations and disorder.

Soon after the discovery of localization, Anderson himself [12] suggested that in real systems lattice deformations could dramatically affect the random potential, possibly leading to a gap opening on the insulating side. Ramakrishnan [3] subsequently argued that, as soon as translational invariance is lost, a direct Hartree-type electron-phonon interaction arises that can strongly renormalize the disorder, reminiscent of charged impurity screening by Coulomb interactions; in contrast with the Coulomb case, however, the lattice deformations should *enhance* (i.e., antiscreen) the effects of disorder. While these early ideas and subsequent works [13–15] strongly emphasized the very significant role of lattice deformations in disordered materials, so far no systematic theory has been put forward that can provide a picture of the resulting MIT.

In this Letter, we present the conceptually simplest theory of disorder-driven MITs, treating Anderson localization at the same level as the electron-phonon interaction. This is achieved by blending typical medium theory (TMT) for Anderson localization [16], and dynamical mean-field theory [4] to tackle lattice deformations. The accuracy of the former has been validated by appropriate cluster extensions, showing it to capture most trends for Anderson transitions [17,18]. Careful systematic studies have also shown the DMFT approach to the electron-phonon problem totally capable of capturing nonperturbative polaronic effects, describing both incoherent self-trapping and coherent quasiparticle properties [19–23].

In clean systems polaron formation occurs only at very strong coupling, uncharacteristic of typical metals. We find that the situation is dramatically different in the presence of sufficient disorder. Here, very pronounced disorder-induced lattice deformations arise in the vicinity of the MIT even in the most common cases of weak or moderate electron-phonon coupling, dominating most observables. It is precisely on such an experimentally relevant region that we concentrate below.

Model and methods.—We study the following disordered Holstein model:

$$H = -t\sum_{\langle ij\rangle} c_i^\dagger c_j + \sum_i \epsilon_i c_i^\dagger c_i - g\sum_i c_i^\dagger c_i X_i + H_{\rm ph}, \quad (1)$$

where $c_i^\dagger$ (c_i) are creation (annihilation) operators for electrons moving on a lattice of sites i with transfer integral t. The site energies ϵ_i are randomly chosen from a uniform distribution of width $2W$, $P_0(\epsilon_i) = \theta(W^2 - \epsilon_i^2)/(2W)$. In addition to the random potential, the electrons interact locally with dispersionless phonons of frequency $\omega_0 = \sqrt{K/M}$ described by $H_{\rm ph} = \sum_i [(KX_i^2)/(2) + (P_i^2)/(2M)]$. The strength of the electron-phonon coupling is measured by the dimensionless parameter $\lambda = g^2/(2KD)$, with D the half bandwidth. As our focus is on metals where electron correlations do not play a major role, we ignore the spin degree of freedom and consider a half-filled band with a semicircular density of states (DOS).

In DMFT for spatially homogeneous systems, the lattice problem Eq. (1) is mapped onto a single impurity which is coupled to the rest of the system via a dynamical Weiss field G_0^{-1} [4]. The latter is determined self-consistently by spatially averaging the local Green's function G over all the equivalent sites of the lattice. While this theory (which in the noninteracting limit is known as the coherent potential approximation, or CPA) can describe certain properties of disordered electron systems on the average [24,25] it does not account for the large and nonnormal fluctuations that cause Anderson localization of the electronic carriers. To this aim an alternative mean-field description can be introduced that focuses on the most probable, or *typical* quantities: the typical density of states (TDOS) is defined as the geometric average of the local DOS over sites with random energy ϵ as $\rho_{\rm typ}(\omega) = \exp\left[\int d\epsilon P_0(\epsilon) \ln \rho(\omega, \epsilon)\right]$. According to the Fermi golden rule, the escape rate from a given site can be estimated as $\tau_{\rm esc}^{-1} \simeq t^2 \rho(\omega, \epsilon)$ [1]; the typical escape rate is therefore proportional to the TDOS, which represents the density of mobile states at a given energy. The region in the band where $\rho_{\rm typ}(\omega)$ vanishes identifies the mobility edge, and its value $\rho_{\rm typ}(0)$ at the Fermi energy serves as an order parameter for the Anderson transition [16].

Solving the full model Eq. (1) involves the calculation of $\Sigma_{e\text{-ph}}(\omega, \epsilon)$, the local electron-phonon self-energy in the presence of site disorder. To this aim we first apply the formulation of Refs. [22,23] where the phonons are represented by a classical field that responds self-consistently to the electrons. The advantage of this method, which is valid in the adiabatic limit $\omega_0/D \to 0$, is that the lattice randomness and the deformations are treated on the same footing, for any value of λ. The effects of phonon quantum fluctuations for $\omega_0 \neq 0$ are subsequently included via a diagrammatic noncrossing approximation (NCA) valid in the weak and moderate electron-phonon coupling regimes [26–28].

Disorder-induced polaron transition and mobility gap.—Figure 1(a) shows the phase diagram obtained from the solution of the TMT-DMFT equations. In the absence of electron-phonon interactions $\lambda = 0$, the theory reduces to that of Ref. [16]: a transition from a metal to an Anderson insulator occurs at a critical disorder strength $W_c^{(0)} = e/2 \simeq 1.36$, identified by $\rho_{\rm typ}(0) = 0$ (all states are localized). Turning the electron-phonon coupling on stabilizes the Anderson insulator, decreasing W_c: as anticipated, the effect is opposite to that of repulsive Coulomb interactions [29] that instead screen out the effects of disorder. As we proceed to show, polaron states characteristic of the strong coupling limit exist all the way down to $\lambda \to 0$, reflecting the positive interplay of disorder and electron-phonon coupling [27,30].

To illustrate the evolution of the electronic properties across the transition, we report in Figs. 2(a)–2(d) both the average DOS and the TDOS, providing, respectively, the spectrum of electronic states and their conductive character. Both quantities, calculated here in the classical phonon limit (Fig. 1 inset), are accessible experimentally through local spectroscopic probes [31]. For strong electron-phonon interactions and weak disorder [panels (a)–(b)], as the electron-phonon coupling strength reaches the critical value λ_c, a mobility gap opens at $\omega = 0$ indicating the

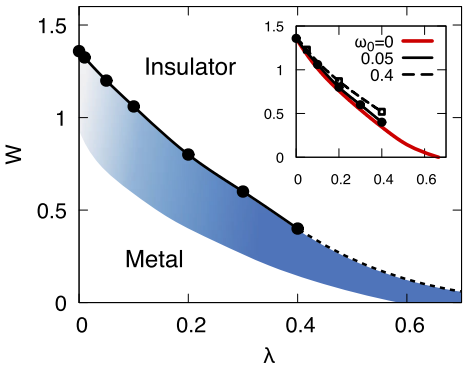

FIG. 1. *Phase diagram.*—Metal-insulator transition (MIT) at $T = 0$ calculated for quantum phonons in the adiabatic regime ($\omega_0 = 0.05$). The shaded area corresponds to the "bad insulator" behavior seen in transport (see text). The dashed line is a sketch of the expected behavior approaching the clean limit. The inset shows the effect of increasing phonon quantum fluctuations.

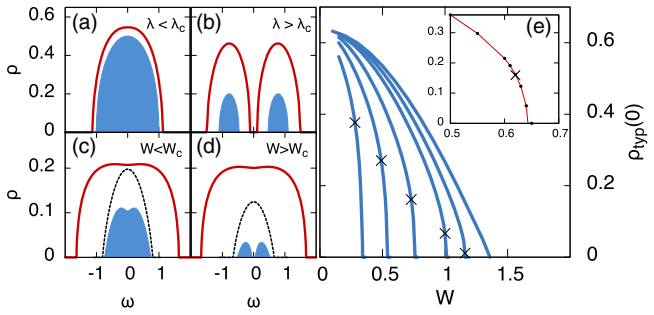

FIG. 2. *Spectral features and order parameter.*—Panels (a)–(d), average (bold line) and typical DOS (shaded) across the MIT at $T = 0$ for classical phonons. (a),(b) at $W = 0.1$, for $\lambda = 0.5, 0.64$; (c),(d) at $\lambda = 0.05$, for $W = 1.1, 1.2$; the dotted line is the TDOS at $\lambda = 0$, shown for comparison; the DOS in the second row have been scaled down by an arbitrary factor for clarity. (e) Order parameter vs disorder amplitude W. From right to left, $\lambda = 0$, 0.05, 0.1, 0.2, 0.3, 0.4. The crosses mark the polaron transition. The inset shows the quantum case for $\lambda = 0.3$ and $\omega_0 = 0.2$.

localization of states around the Fermi energy (TDOS, shaded). This is rapidly followed by the disappearance of the states themselves (DOS, red), as both phenomena are driven by polaron formation: self-trapping of the charges due to strong electron-phonon interactions (and pinned by weak disorder) leads to a binary distribution of lattice displacements that splits the excitation spectrum into two separate subbands [22].

Strikingly, the opening of a mobility *gap* at the MIT persists down to the weakly interacting limit, a situation that is of broad relevance to many disordered materials. The behavior observed as the transition line is crossed upon increasing W at small λ [cf. Fig. 2(d)] is fundamentally different from the case where lattice effects are ignored from the beginning, where all states become localized at the MIT and no mobility gap is observed (dotted line). At variance with the strong electron-phonon coupling limit, however, here the mobility gap opens at the Fermi energy in an electronic spectrum that is otherwise essentially unperturbed. The critical behavior of the order parameter, shown in Fig. 2(e), is also modified accordingly: the mean-field behavior $\rho_{\rm typ} \sim (W_c - W)$ found at $\lambda = 0$ [16] changes to $(W_c - W)^{1/2}$ at the approach of the MIT, indicating a radical change in the disorder distribution as soon as $\lambda \neq 0$ [32].

Self-consistent local potentials.—To substantiate this statement, we introduce the self-consistent field $u = \epsilon + {\rm Re}\Sigma_{e\text{-ph}}(\omega = 0, \epsilon)$, defined as the local energy level renormalized by the interaction with the deformable lattice. In the static phonon limit considered first, the real part of the electron-phonon self-energy reduces at $T = 0$ to the energy-independent Hartree term ${\rm Re}\Sigma(\omega, \epsilon) = \sqrt{\lambda} X_0(\epsilon)$, where $X_0(\epsilon)$ is the static local deformation on a site, given the local potential ϵ [22]. It is clear from Eq. (1) that the site disorder acts as a polarization field coupled to the charge, in full analogy with the external magnetic field in the Ising model. Accordingly, an order parameter for the polaron transition can be defined as the value $X_0 = \lim_{\epsilon \to 0^+} X_0(\epsilon)$ much like the remnant magnetization in a ferromagnet, as shown in Fig. 3(a).

Inverting for $\epsilon(u)$ leads to the effective disorder distribution $P_{\rm eff}(u) = P_0[\epsilon(u)]/|1 + [(\partial \Sigma_{e\text{-ph}})/(\partial \epsilon)]|$ reported in Fig. 3(b), showing that the action of the lattice degrees of freedom dramatically changes the nature of the disorder. As randomness increases, the presence of correlated electron-lattice displacements leads to a discontinuity in $X_0(\epsilon)$, signaling a polaron transition; correspondingly, a gap opens in $P_{\rm eff}(u)$. Moreover, the buildup of local deformations correlated with the large fluctuations of the site potentials starts already well before the transition, This causes a dip in the distribution [dashed line in Fig. 3(b)] and a suppression of the mobile states available at the Fermi energy [Fig. 2(c)], which has fundamental consequences for charge transport as we show next.

Minimum metallic conductivity.—We evaluate the electrical conductivity from the Kubo formula following Refs. [33,34], by expressing the current-current correlation function as $\chi_{JJ}(\omega) = \Lambda(\omega) P_1(\omega)$, which isolates the dominant nonlocal contribution P_1 responsible for localization. From Ref. [25] we have that $P_1(\omega) = B(\omega)\rho_{\rm typ}(\omega)$ with $B(\omega)$ a weakly ω-dependent function, so that the conductivity is correctly proportional to the order parameter of the Anderson transition. The prefactor Λ is noncritical and can be calculated within DMFT-CPA as $\Lambda(\omega) = \chi^{\rm CPA}_{JJ}(\omega)/P^{\rm CPA}_1(\omega)$, leading to the following interpolation formula (see Supplemental Material [35]):

$$\sigma = \sigma_0 \int d\omega \left(-\frac{\partial f}{\partial \omega}\right) \frac{\chi^{\rm CPA}_{JJ}(\omega)}{\rho(\omega)} \rho_{\rm typ}(\omega), \qquad (2)$$

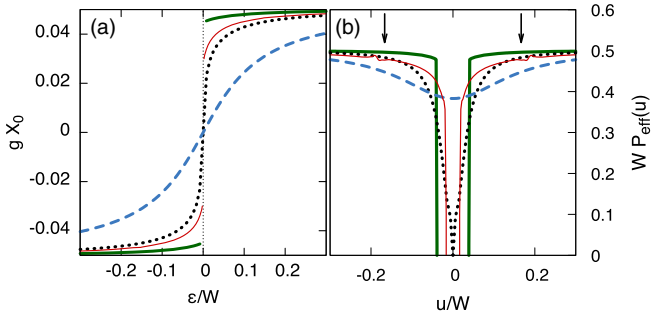

FIG. 3. *Self-consistent fields and effective disorder.*—(a) Lattice displacement X_0 as a function of ϵ and (b) effective disorder distribution: below ($W = 1.0$, dashed), at ($W = 1.15$, dotted) and beyond the polaronic transition ($W = 1.2$, bold), for $\lambda = 0.05$ and $T = 0$. Thin lines in (a) and (b) are the NCA results for quantum phonons at $W = 1.2$ and $\omega_0 = 0.2$ [the value of ω_0 is marked by arrows in (b)].

where f is the Fermi function and $\sigma_0 = \pi e^2 a^2/\hbar v$ the conductivity unit (a and v are, respectively, the lattice parameter and the unit cell volume). Equation (2) can be greatly simplified by taking the $T \to 0$ limit and introducing the transport scattering time from the semiclassical expression $\chi_{JJ}^{\mathrm{CPA}}(0) \propto \rho(0)\tau$ [21]. The resulting

$$\sigma \propto \rho_{\mathrm{typ}}(0)\tau \tag{3}$$

acquires a transparent physical meaning: upon approaching the Anderson insulator, part of the carriers localize due to quantum interference effects and drop out of the conductivity, which is encoded in ρ_{typ} [1]; the remaining itinerant carriers are not affected by localization and are, therefore, scattered by disorder and lattice fluctuations in a way that is properly described by the semiclassical τ.

The conductivity obtained from Eq. (2) is illustrated in Fig. 4(a) [note that Eq. (3) would provide essentially indistinguishable results for $T \lesssim 0.1$]. Within the metallic regime at low disorder, the standard Drude-Boltzmann picture applies, leading to a conductivity that decreases with temperature. This is due to strongly temperature-dependent scattering between (largely) T-independent electronic states. This can be checked directly in Fig. 4(b), which reports the behavior of τ and ρ_{typ} separately. Upon increasing the disorder strength, the scattering rate progressively increases (τ decreases) until it becomes comparable with the bandwidth D, cf. Fig. 4(c). At this point, denoted as $W = W^*$, all quantities including the conductivity become essentially temperature independent. For even stronger disorder, the scattering time cannot be reduced further, as it has already saturated to its minimum value.

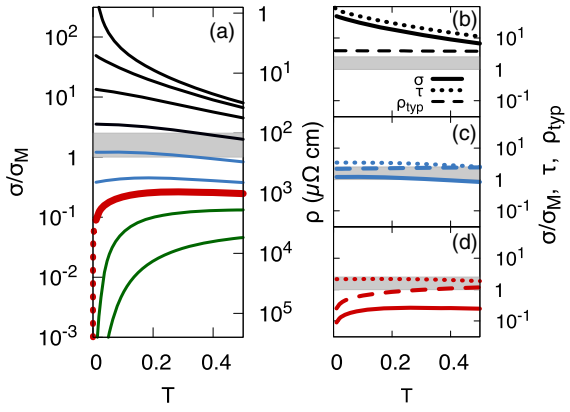

FIG. 4. *Conductivity and Mott limit.*—(a) $\sigma(T)$ in the weak-coupling regime, $\lambda = 0.05$, expressed in units of σ_M (see text); from top to bottom, $W = 0.0$, 0.125, 0.25, 0.5; 0.8, 1.05, 1.16, 1.3, 1.5. For $W = W_c = 1.16$ (bold) we also show the power-law extrapolation to $T = 0$ (dotted). The shaded area is the experimental range 100–250 $\mu\Omega$ cm where the TCR is seen to vanish in most single-band materials [36,37]. (b)–(d) Scattering time and order parameter for representative parameters in the metallic phase ($W = 0.125$), at the Mott-Ioffe-Regel limit ($W = W^* = 0.8$) and at the MIT ($W = W_c$). Both quantities are expressed in units of $1/D$.

Remarkably, the value of the conductivity at W^* precisely coincides with Mott's minimum metallic conductivity σ_M, i.e., the Mott-Ioffe-Regel (MIR) limit [37–39]. The MIR limit therefore marks the onset of a regime where transport is not governed by how the electrons are scattered, but rather by the strong T dependence of the electronic spectrum itself: a mobility pseudogap opens at low T reflecting disorder-enhanced polaronic processes [cf. Fig. 2(c) and the subsequent discussion], which is progressively filled upon increasing the temperature as shown in Fig. 4(d) (dashed line). Moreover, the actual number of mobile charge carriers is much smaller than the total number of electrons in the system, as most electronic states are now localized. This results in a "bad insulator" transport regime (Fig. 4, blue and Fig. 1, shaded) which displays conductivity values below the MIR limit and an insulatinglike temperature coefficient $d\sigma/dT > 0$ but with a finite DC intercept, an unexplained behavior that is often observed in strongly disordered metals [3]. Such an intermediate regime ends at the critical point, where a mobility gap fully opens and the conductivity eventually vanishes at $T = 0$ (thick line).

Lattice quantum fluctuations.—We now show that the MIT reported in Fig. 1 is a robust phenomenon; i.e., a genuine transition exists from $\omega_0 = 0$ all the way to $\omega_0 \to \infty$. The critical line obtained in the static limit is shown in the inset of Fig. 1. In the opposite limit, $\omega_0 \to \infty$ (λ finite), the electron-phonon interaction becomes ineffective for spinless electrons. The transition therefore occurs at the noninteracting value $W_c^{(0)}$ independent of λ. We conclude that a MIT must exist for any finite ω_0, located between $W_c^{(0)}$ and the critical line for classical phonons. This is indeed what we find numerically [Figs. 1 and 2(e), insets]. Increasing values of ω_0 produce a slight stabilization of the metal; yet, at the coupling strengths attainable with the NCA, the MIT remains very close to the one calculated with classical phonons. Sizable differences are expected instead as one approaches the clean limit $W = 0$. There, it is known that quantum fluctuations push the MIT to $\lambda \to \infty$, while the classical limit yields a transition at $\lambda_c^{(0)} = 0.67$ [22]. A sketch of the behavior inferred from the above considerations is shown as a dashed line in Fig. 1.

The key phenomenon that we unveiled, i.e., the correlated response of the lattice to the local random potentials, is also preserved at finite ω_0: as shown in Fig. 3(b), the distribution of the self-consistent field is essentially unchanged by phonon quantum fluctuations at large ϵ, and the gap in the distribution of u remains finite, although somewhat renormalized as compared to the static phonon case. In more refined treatments, such a gap could be partially filled by exponential tails [26,40,41].

Concluding remarks.—In this Letter, we provided a clear microscopic picture of disorder-driven MITs in deformable

lattices, where disorder-enhanced interaction effects dominate all physical processes. Such interplay is revealed most prominently in the emergence of an intermediate regime that separates the conventional metal from the insulator, where the system still conducts at $T = 0$, but it displays resistivity that *decreases* with temperature, i.e., negative TCR behavior. Remarkably, the boundary of this anomalous transport regime, found at intermediate disorder $W = W^*$, is marked precisely by the resistivity reaching the Mott-Ioffe-Regel limit, as argued in very early works by Mott. The actual MIT point is reached at somewhat stronger disorder $W = W_c > W^*$, and it displays all signatures of a $T = 0$ quantum critical point, with power-law scaling behavior of all quantities. Our findings, therefore, reconcile Mott's concept of "minimum metallic conductivity," and the ideas based on the scaling theory of localization of Anderson and followers. We showed that both ideas apply, but they do so in two physically distinct regimes within the phase diagram. Our results open the road to properly interpret many puzzling experiments in disordered metals, including the long-standing puzzle of "Mooij correlations" [3,36], which remains a challenge for future work.

V. D. was supported by the NSF Grant No. DMR-1410132. D. D. S. acknowledges the German Research Foundation (DFG-SFB 1170). S. C. and D. D. S. acknowledge CINECA ISCRA-C HPC Project No. HP10C5W99T and the SuperMUC system at the Leibniz Supercomputing Centre under the Project-ID pr94vu.

[1] P. W. Anderson, Phys. Rev. **109**, 1492 (1958).
[2] F. Evers and A. D. Mirlin, Rev. Mod. Phys. **80**, 1355 (2008).
[3] P. A. Lee and T. V. Ramakrishnan, Rev. Mod. Phys. **57**, 287 (1985).
[4] A. Georges, G. Kotliar, W. Krauth, and M. J. Rozenberg, Rev. Mod. Phys. **68**, 13 (1996).
[5] E. Miranda and V. Dobrosavljevic, Rep. Prog. Phys. **68**, 2337 (2005).
[6] A. A. Pastor and V. Dobrosavljević, Phys. Rev. Lett. **83**, 4642 (1999).
[7] V. Dobrosavljević and G. Kotliar, Phys. Rev. Lett. **78**, 3943 (1997).
[8] Z. Fisk and G. W. Webb, Phys. Rev. Lett. **36**, 1084 (1976).
[9] T. Siegrist, P. Jost, H. Volker, M. Woda, P. Merkelbach, C. Schlockermann, and M. Wuttig, Nat. Mater. **10**, 202 (2011).
[10] N. F. Mott, *Metal-Insulator Transition* (Taylor & Francis, London, 1990).
[11] V. Dobrosavljević, N. Trivedi, and J. M. Valles Jr., *Conductor Insulator Quantum Phase Transitions* (Oxford University Press, Oxford, 2012).
[12] P. W. Anderson, Nature (London), Phys. Sci. **235**, 163 (1972).
[13] H. Shore, L. Sander, and L. Kleinman, Nature (London), Phys. Sci. **245**, 44 (1973).
[14] M. H. Cohen, E. N. Economou, and C. M. Soukoulis, Phys. Rev. Lett. **51**, 1202 (1983).
[15] Y. Shinozuka, J. Non-Cryst. Solids **77–78**, 21 (1985).
[16] V. Dobrosavljević, A. A. Pastor, and B. K. Nikolić, Europhys. Lett. **62**, 76 (2003).
[17] C. E. Ekuma, H. Terletska, K.-M. Tam, Z.-Y. Meng, J. Moreno, and M. Jarrell, Phys. Rev. B **89**, 081107 (2014).
[18] Y. Zhang, H. Terletska, C. Moore, C. Ekuma, K.-M. Tam, T. Berlijn, W. Ku, J. Moreno, and M. Jarrell, Phys. Rev. B **92**, 205111 (2015).
[19] S. Ciuchi, F. de Pasquale, S. Fratini, and D. Feinberg, Phys. Rev. B **56**, 4494 (1997).
[20] S. Fratini and S. Ciuchi, Phys. Rev. Lett. **91**, 256403 (2003).
[21] A. J. Millis, J. Hu, and S. Das Sarma, Phys. Rev. Lett. **82**, 2354 (1999).
[22] A. J. Millis, R. Mueller, and B. I. Shraiman, Phys. Rev. B **54**, 5389 (1996).
[23] S. Ciuchi and F. de Pasquale, Phys. Rev. B **59**, 5431 (1999).
[24] R. Alben, M. Blume, H. Krakauer, and L. Schwartz, Phys. Rev. B **12**, 4090 (1975).
[25] A. Alvermann, F. X. Bronold, and H. Fehske, Phys. Status Solidi C **1**, 63 (2004).
[26] M. Capone and S. Ciuchi, Phys. Rev. Lett. **91**, 186405 (2003).
[27] D. Di Sante and S. Ciuchi, Phys. Rev. B **90**, 075111 (2014).
[28] Y. F. Nie, D. Di Sante, S. Chatterjee, P. D. C. King, M. Uchida, S. Ciuchi, D. G. Schlom, and K. M. Shen, Phys. Rev. Lett. **115**, 096405 (2015).
[29] M. C. O. Aguiar, V. Dobrosavljević, E. Abrahams, and G. Kotliar, Phys. Rev. Lett. **102**, 156402 (2009).
[30] G. Sangiovanni, P. Wissgott, F. Assaad, A. Toschi, and K. Held, Phys. Rev. B **86**, 035123 (2012).
[31] A. Richardella, P. Roushan, S. Mack, B. Zhou, D. A. Huse, D. D. Awschalom, and A. Yazdani, Science **327**, 665 (2010).
[32] S. Mahmoudian, S. Tang, and V. Dobrosavljević, Phys. Rev. B **92**, 144202 (2015).
[33] S. M. Girvin and M. Jonson, Phys. Rev. B **22**, 3583 (1980).
[34] R. Abou-Chacra, D. J. Thouless, and P. W. Anderson, J. Phys. C **6**, 1734 (1973).
[35] See Supplemental Material at http://link.aps.org/supplemental/10.1103/PhysRevLett.118.036602 for the derivation of the interpolation formula Eq. (2).
[36] C. C. Tsuei, Phys. Rev. Lett. **57**, 1943 (1986).
[37] N. Hussey, K. Takenaka, and H. Takagi, Philos. Mag. **84**, 2847 (2004).
[38] O. Gunnarsson, M. Calandra, and J. E. Han, Rev. Mod. Phys. **75**, 1085 (2003).
[39] We define the Mott limit σ_M, as usual, as the value of the Drude conductivity when the mean-free-path ℓ equals the lattice spacing a. In a cubic lattice, this corresponds to a scattering rate $\hbar/\tau = D/3$. For a concentration $x = 1/2$ of spinless electrons as considered in this work we obtain in our units $\sigma_M = \sigma_0/(2\pi)$. The conductivity σ_0 is fixed by taking a representative value $a = 3$ Å.
[40] P. Benedetti and R. Zeyher, Phys. Rev. B **58**, 14320 (1998).
[41] M. Capone, P. Carta, and S. Ciuchi, Phys. Rev. B **74**, 045106 (2006).